Stability after confinement of the H atom

M. F. Morcillo, E. F. Borja, J. M. Alcaraz-Pelegrina and A. Sarsa*

Departamento de Física, Campus de Rabanales, Edif. C2. Universidad de Córdoba, E-14071 Córdoba, Spain

Abstract

The stability of a spherically confined atomic system when confinement is removed is studied. We consider s, p, d and f states of the Hydrogen atom confined by a finite barrier. The stability is characterised in terms of the ionisation probability of the atom when confinement is removed. The ionisation probability presents different sharply peaked, non-symmetric maxima as a function of the confinement radius that can be explained in terms of tunnelling and re-tunnelling of the confined bound states. The spatial structure of the confined bound state plays a key role in the stability of the atom. Different measures arising from information theory, such as information entropy, disequilibrium indices and complexity measures, have been calculated to characterise quantitatively the structure of the confined state. A direct relationship between the complexity of a confined state and its stability when it is released from confinement has been found.

Keywords: confined atoms, electronic structure, ionisation probability, sudden approximation, statistical complexity

1. Introduction

The experimental achievement of inserting atoms and molecules in molecular nanocontainers [1, 2, 3] has increased the interest in these complexes. Different applications of these structures have been proposed for energy transport and storage [4] or in medicine [5, 6]. Spatial confinement leads to a modification of the properties of enclosed species as, for example, the energy levels. Absorption and emission properties can be modified by the confinement, see e.g. [7], so encapsulated atoms present interesting applications

*Corresponding author: A. Sarsa. Email: fa1sarua@uco.es

because they open the possibility of designing materials with selected optical properties [8].

The bound state properties of encapsulated atoms and molecules have been widely studied in the literature, see e.g. the reviews [9, 10, 11, 12]. However, the knowledge of stability after confinement is much more scarce [13, 14]. This aspect is important because many of the above mentioned applications are based, first, on inserting the atom or molecule of interest into a molecular cavity, and second, on extracting it for its future use. This requires that the atom remains stable when confinement is removed, which is not necessarily the case because spatial confinement changes the energy of the encapsulated atom with respect to its value when no confinement is present. This leads to a probability of ionisation or dissociation of the atom or molecule when it is extracted from the cage.

In this work we address the problem of the stability of an atom when it is released from confinement. The ionisation probability is calculated for different initial states and confining sizes. We consider a penetrable repulsive spherically symmetric model for confinement which contains relevant physical features of spatial confinement [15, 16]. We study the excited states of the Hydrogen atom, for which a very accurate analysis can be carried out and it provides the basis for the understanding of this process for more complex systems. The sudden approximation is employed for calculating the time evolution of the atomic state when it is released from confinement. The results have been analysed in terms of energy and confined orbitals shell structure that plays a key role in the stability of the atom when it is released from confinement. The structure of the charge distribution is characterised in terms of quantitative measures of the complexity of the electronic density. The complexity is related to the information content, uncertainty or delocalisation of the electronic charge distribution. In Quantum Chemistry, several definitions of complexity have been applied to analyse different properties and processes related to structure studies and reactivity [17]. Atomic units are used through out this work.

2. Methodology

We start from a confined atom in a stationary state, $\Psi^{\rm c}_{nlm}$,

$$H^{\rm c}\ \Psi^{\rm c}_{nlm}(\vec{r}) = E^{\rm c}_{nl}\ \Psi^{\rm c}_{nlm}(\vec{r}) \tag{1}$$

where $H^{\rm c}$ is the Hamiltonian of the confined Hydrogen atom

$$H^{\rm c} = -\frac{1}{2}\nabla^2 - \frac{1}{r} + v_c(r), \tag{2}$$

and $v_c(r)$ is the confining potential

$$v_c(r) = \begin{cases} v_0 & \text{if} \quad r_0 \leq r \leq r_0 + \Delta \\ 0 & \text{otherwise,} \end{cases} \tag{3}$$

with r_0 the inner radius, v_0, the height, and Δ, the width of the barrier. Here, we use $v_0 = 2.5$ and $\Delta = 5$, as in [16]. The wave function of the confined state can be written as

$$\Psi^{\rm c}_{nlm}(\vec{r}) = \frac{u^{\rm c}_{nl}(r)}{r} Y_{lm}(\Omega). \tag{4}$$

When the atom is extracted from the confining cavity, the Hamiltonian reduces to that of the free Hydrogen atom. The wave function of the atom when it is released from confinement can be expanded in terms of the stationary states of the free Hydrogen atom

$$\Psi^{\rm f}_{lm}(\vec{r}, t) = \sum_{n'=0}^{\infty} C^{nl}_{n'} e^{-iE_{n'}\,t} \Psi_{n'lm}(\vec{r}) + \int_0^{\infty} dE\, C^{nl}(E) e^{-iE\,t} \Psi_{Elm}(\vec{r}). \tag{5}$$

Note that, due to the spherical symmetry of the confining potential, l and m do not change when confinement is removed.

If we assume that one can neglect the time to extract the atom from the confining cavity, then

$$C^{nl}_{n'} = \int_0^{\infty} dr\; u_{n'l}(r) u^{\rm c}_{nl}(r), \quad C^{nl}(E) = \int_0^{\infty} dr\; u_{El}(r) u^{\rm c}_{nl}(r), \tag{6}$$

where $u_{n'l}(r)$ and $u_{El}(r)$ are the reduced radial functions of the bound and ionised Hydrogen states, respectively. The bound states are normalized to one and the states of the continuum spectrum are normalized in the energy scale. When confinement is removed, $|C^{nl}_{n'}|^2$ gives the probability that the electron lies in the $\{n'lm\}$ bound state of the free atom, and $|C^{nl}(E)|^2 dE$ is the probability that the electron is ejected with energy between E and $E + dE$. The total ionisation probability is calculated as

$$P_{\rm I} = \int_0^{\infty} dE\, |C^{nl}(E)|^2, \tag{7}$$

and the probability that the atom is not ionised as

$$P_{\rm B} = \sum_{n'=0}^{\infty} |C_{n'}^{nl}|^2 = 1 - P_{\rm I}. \tag{8}$$

The reduced radial functions are computed here by using the analytic continuation method [18, 19, 20]. This technique is based on a polynomial expansion of the solution around each one of the tabular points. The interaction potential is also expanded in a power series around these points. The linear coefficients of the solution at each point are obtained through a three term recursion relation. By using step sizes of 10^3 and polynomials of range 20, very accurate solutions of the radial Schrödinger equation are obtained. The calculation of the integrals giving the C coefficients, Eq. (6), can be done analytically by using the piecewise polynomial representation of the reduced radial function.

Quantitative analysis of complexity are based on measure indices which provide different information about the confined system. These indices can be written as the product of two terms, one related to the disequilibrium from the most probable state and the other to the information content of the system. In particular, we consider complexity measures proposed by López-Ruiz, Mancini and Calbet [21] (LMC) in its shape complexity form [22], and the Fisher-Shannon complexity [23] (FS). Information, delocalisation and complexity indices have been employed to quantitatively study the importance of the shape and structure of the electronic charge distribution of different properties [17] and effects as for example relativistic [24] and confinement effects [25, 26].

The shape form of the LMC index in position space is defined as

$$C_r^s = D_r H_r, \tag{9}$$

where D_r is the disequilibrium function given by the density expectation value

$$D_r = \int d\vec{r}\, \rho^2(r), \tag{10}$$

with $\rho(r)$ the spherically averaged electron density distribution normalized to unity. D_r is related to the distance from the most probable state, the equilibrium, which within this framework is the uniform density.

H_r is a measure of the information of the state and it is defined as

$$H_r = e^{S_r} \tag{11}$$

where S_r is the Shannon information entropy

$$S_r = -\int d\vec{r}\, \rho(r) \ln \rho(r). \tag{12}$$

On the other hand, the FS index is, in position space,

$$P_r = I_r \frac{1}{2\pi e} H_r^{\frac{2}{3}}, \tag{13}$$

with the Fisher information measure, I_r, as

$$I_r = \int d\vec{r}\, \frac{|\vec{\nabla}\rho(r)|^2}{\rho(r)}. \tag{14}$$

This is another measure for the distance from the most probable state.

3. Results and discussion

In Figure 1, we plot the energy of the confined $2p-5p$ states as a function of r_0. It is negative and presents a sawtooth structure. Each np orbital energy has $n-1$ local maxima whose positions coincide with the positions of the local minima of the $(n+1)p$ orbital energy.

Figure 1

The physical origin of these kinks lies in the behaviour of the orbitals around some critical values of the confinement radius r_0. This is studied in Figure 2, where we plot in the upper panel, the $4p$ orbital obtained for $r_0 = 25.15$ and $r_0 = 25.20$. The unconfined orbital, i.e. without the penetrable barrier, is also plotted for the sake of comparison.

Figure 2

For $r_0 = 25.20$ the $4p$ state is within the confinement region. A small decrease of the confinement size, $r_0 = 25.15$, leads to an abrupt change in the structure of the orbital, which becomes negligible inside the cavity. The nodes of the $4p$ orbital for $r_0 = 25.15$ are not visible within the scale of the figure. The orbital has tunnelled out when the confinement radius has been reduced. Although the charge distribution is very different in both situations, the energy of the $4p$ orbital is very similar. In fact, the orbital energy is continuous as a function of the cavity size, as it can be seen in Figure 1. The behaviour of the $5p$ orbital, see the lower panel of Figure 2, is the opposite to that of the $4p$ orbital. For $r_0 = 25.20$ it lies outside the

confinement region while for $r_0 = 25.15$ it is within the confinement region. The $4p$ orbital leaves the cavity for the r_0 where the $5p$ orbital tunnels in. The energy of both orbitals for that particular r_0 value is very similar and corresponds to a local maximum and a local minimum of the $4p$ and $5p$ orbital energies respectively. The behaviour of the orbital energy as a function of r_0 is related to the phenomena of the avoided crossing: neighbouring levels with the same symmetry repel each other when they become close and do not cross. This behaviour has been also obtained for d, f, ... confined orbitals here studied and it was previously found for the s orbitals [14] and for S states of the confined He atom in a spherical potential well [27].

The energy of the nl orbital as a function of r_0 presents a sawtooth structure with $n-l$ local maxima, as shown in Figure 3 for the orbitals of the N shell of the Hydrogen atom. If one starts the analysis from the unconfined situation, $r_0 \to \infty$, when smaller r_0 values are considered, the states that tunnel out first are those whose orbital quantum number is smaller. The local maxima of the $4s$ orbital appear for lager r_0, followed by the local maxima of the $4p$, $4d$ and $4f$ states. The reason is that their spatial extension is larger and they are affected by confinement at bigger values of r_0.

Figure 3

The behaviour of the confined orbitals with the cavity size has an effect on the ionisation probability when the atom is released from confinement. In previous studies [13], we have obtained that the ionisation probability does not depend directly on the energy of the confined state as one could think beforehand. The spatial structure of the radial function of the confined orbital, and in particular the location and extension of the electronic shells, governs the ionisation probability.

Figure 4

In Figure 4 we plot the ionisation probabilities for the $2p$ to $5p$ states as a function of r_0. An oscillatory behaviour with several sharply peaked, non-symmetric maxima are found for those r_0 values where the states tunnel. When the state is within the confinement region, the ionisation probability increases as r_0 decreases, while an oscillatory behaviour is observed when the state is outside the confinement region. The ionisation probability presents a counterintuitive behaviour when the state tunnels. A steep rise in the ionisation probability is observed when the orbital enters into the confinement region. The energy of the orbital is practically unchanged when the orbital tunnels in, but the slope sign of the energy as a function of r_0 changes. The ionisation probability is governed by the structure of the charge distribution.

Information theoretical tools are employed to study quantitatively the structure of the confined orbitals. The complexity indices here employed, Eqs. (9) and (13), include both the delocalisation and the information content of the charge density. For sake of space we only report here results for the N shell, which are representative for the rest of cases.

In Figure 5, we plot the disequilibrium function, D_r, Eq. (10), and the Fisher information measure, I_r, Eq. (14), for the $4s$ to $4f$ orbitals as a function of r_0. Both indices present a similar pattern characterised by maxima in the regions where states are confined inside the barrier. This is due to the compression of the electronic charge towards the nucleus which leads to both, a more compact density and a larger curvature of the radial functions. On the other hand, these indices practically vanish when the states tunnel out because their spatial extension is larger, the curvature decreases and the density is more uniform inducing a minimum disequilibrium.

Figure 5

In Figure 6, we plot the exponential Shannon entropy, H_r, Eq. (11), as a function of the confinement size. This index provides a measure of the information of the state. Unlike disequilibrium indices, if states are confined between the origin and the wall, their uncertainty in position drops and small H_r is obtained. The opposite holds when orbitals lie mostly outside the barrier, the uncertainty in the position is higher and the value of the information index is larger.

Figure 6

Complexity indices contain both, disequilibrium and information measures simultaneously. Both indices present opposite behaviours when the charge is localised inside or outside the confinement region. The complexity indices here studied are governed by the disequilibrium as shown in Figure 7, where we plot the LMC shape complexity measure, C_r^s, Eq. (9), and the FS index, P_r, Eq. (13), as a function of r_0. When the states are inside the cage, the larger value of disequilibrium index compensates for the lower information content. Outside the confinement region, although the information index is large, the low values of the disequilibrium lead to a smaller complexity of the state. As a result the complexity indices are sensitive to the structure of the orbitals and present the same structure as the ionisation probability. The states are more complex when they are localised inside the confinement region and the complexity grows as the confinement volume is reduced. When the state jumps out of the confinement region a sharp drop in the complexity is observed. In the light of these results, complexity indices

and other information theory measures characterise avoided level crossing, tunnelling of confined states and the stability of the atom when confinement is removed.

Figure 7

4. Conclusions

The stability of a Hydrogen atom when confinement is removed is studied in terms of the ionisation probability of the confined states. A penetrable spherical barrier is used as a model for confinement. The confined atom is initially in a stationary state and the time needed to extract the atom is assumed to be small. The ionisation probability of each nl state as a function of the confinement size presents an oscillatory behaviour with $n - l$ sharply peaked, non-symmetric maxima. This behaviour has been explained in terms of successive tunnelling and re-tunnelling processes through the barrier at different inner radii. This is also reflected in the energy and its sawtooth structure, where the maxima are located at the same radii as those of the ionisation probability.

The shape LMC and the FS complexity measures have also been calculated. Confinement effects on these indices have been studied. The value of the disequilibrium governs the behaviour of the complexity of the confined state. The larger value of the disequilibrium indices of the states when the charge is localised within the confinement barrier overcomes the lower information content of the state. Our calculations show that complexity is a measure of the stability of the confined atom when it is released from confinement: the larger the complexity the smaller its stability. The complexity, as well as the ionisation probability, are greatly reduced when the electronic charge distribution of the confined state lies mostly outside the confinement region. This particular charge distribution appears when the confined bound state has tunnelled out the penetrable confining barrier.

Acknowledgements

This work was partially supported by the Spanish Dirección General de Investigación Científica y Técnica (DGICYT) and FEDER under contract FIS2015-69941-C2-2-P and the Junta de Andalucía under grant FQM378. M.F.M. acknowledges partial support by a Ph.D fellowship from the Spanish Ministerio de Ciencia, Innovación y Universidades under grant FPU16/05950.

References

[1] K. Komatsu, M. Murata, Y. Murata, Encapsulation of molecular hydrogen in fullerene C_{60} by organic synthesis, Science 307 (2005) 238.

[2] A. J. Horsewill, K. S. Panesar, S. Rols, M. R. Johnson, Y. Murata, K. Komatsu, S. Mamone, A. Danquigny, F. Cuda, S. Maltsev, M. C. Grossel, M. Carravetta, M. H. Levitt, Quantum translator-rotator: Inelastic neutron scattering of dihydrogen molecules trapped inside anisotropic fullerene cages, Physical Review Letters 102 (2009) 013001.

[3] A. Krachmalnicoff, R. Bounds, S. Mamone, S. Alom, M. Concistre, B. Meier, K. Kouril, M. E. Light, M. R. Johnson, S. Rols, A. J. Horsewill, A. Shugai, U. Nagel, T. Room, M. Carravetta, M. H. Levitt, R. J. Whitby, The dipolar endofullerene HF@C60, Nature Chemistry 8 (2016) 953.

[4] K. Ayub, Transportation of hydrogen atom and molecule through $X_{12}Y_{12}$ nano-cages, International Journal Of Hydrogen Energy 42 (2017) 11439.

[5] D. W. Cagle, S. J. Kennel, S. Mirzadeh, J. M. Alford, L. J. Wilson, In vivo studies of fullerene-based materials using endohedral metallofullerene radiotracers, Proceedings of the National Academy of Sciences 96 (1999) 5182–5187.

[6] T. Li, H. C. Dorn, Biomedical applications of metalencapsulated fullerene nanoparticles, Small 13 (2017) 1603152.

[7] R. Cabrera-Trujillo, Sum rules and the role of pressure on the excitation spectrum of a confined hydrogen atom by a spherical cavity, Journal of Physics B: Atomic, Molecular and Optical Physics 50 (2017) 155006.

[8] M. Anaya, A. Rubino, T. C. Rojas, J. F. Galisteo-López, M. E. Calvo, H. Míguez, Strong quantum confinement and fast photoemission activation in $CH_3NH_3PbI_3$ perovskite nanocrystals grown within periodically mesostructured films, Advanced Optical Materials 5 (2017) 1601087.

[9] W. Jaskolski, Confined many-electron systems, Physics Reports 271 (1996) 1.

[10] J. Sabin, E. Brändas, S. Cruz (Eds.), Theory of Confined Quantum Systems, Advances in Quantum Chemistry Vol. 57–58, Elsevier, Oxford, UK, 2009.

[11] K. D. Sen (Ed.), Electronic Structure of Quantum Confined Atoms and Molecules, Springer-Verlag, Switzerland, 2014.

[12] E. Ley-Koo, Recent progress in confined atoms and molecules: Superintegrability and symmetry breakings, Rev. Mex. Fis. 64 (2018) 326–363.

[13] M. F. Morcillo, J. M. Alcaraz-Pelegrina, A. Sarsa, Ionization probability of the hydrogen atom suddenly released from confinement, International Journal of Quantum Chemistry 118 (2018) e25563.

[14] M. F. Morcillo, J. M. Alcaraz-Pelegrina, A. Sarsa, Ionisation and excitation probabilities of a hydrogen atom suddenly released from penetrable confinement, Molecular Physics (2019) 1–8. doi:10.1080/00268976.2018.1547429.

[15] J.-P. Connerade, V. K. Dolmatov, P. A. Lakshmi, The filling of shells in compressed atoms, Journal of Physics B: Atomic, Molecular and Optical Physics 33 (2000) 251–264.

[16] V. K. Dolmatov, J. L. King, Atomic swelling upon compression, Journal of Physics B: Atomic, Molecular and Optical Physics 45 (2012) 225003–1–225003–5.

[17] K. D. Sen (Ed.), Statistical Complexity, Applications in Electronic Structure, Springer, London, 2011.

[18] A. Holubec, A. D. Stauffer, Efficient solution of differential equations by analytic continuation, Journal of Physics A: Mathematical and Theoretical 18 (1985) 2141.

[19] R. J. W. Hodgson, Precise shooting methods for the schrodinger equation, Journal of Physics A: Mathematical and Theoretical 21 (1988) 679.

[20] E. Buendía, F. J. Gálvez, A. Puertas, Study of the singular anharmonic potentials by means of the analytic continuation method, Journal of Physics A: Mathematical and Theoretical 28 (1995) 6731.

[21] R. López-Ruiz, H. L. Mancini, X. Calbet, A statistical measure of complexity, Physics Letters A 209 (1995) 321–326.

[22] R. G. Catalán, J. Garay, R. López-Ruiz, Features of the extension of a statistical measure of complexity to continuous systems, Physical Review E 66 (2002) 011102.

[23] J. C. Angulo, J. Antolín, K. D. Sen, Fisher-shannon plane and statistical complexity of atoms, Physics Letters A 372 (2008) 670–674.

[24] P. Maldonado, A. Sarsa, E. Buendía, F. Gálvez, Relativistic effects on complexity indexes in atoms in position and momentum spaces, Physics Letters A 374 (2010) 3847.

[25] M. Rodríguez-Bautista, R. Vargas, N. Aquino, J. Garza, Electron-density delocalization in many-electron atoms confined by penetrable walls: A Hartree-Fock study, International Journal of Quantum Chemistry 143 (2018) e25571.

[26] W. Nascimento, F. Prudente, Shannon entropy: A study of confined hydrogenic-like ions, Chemical Physics Letters 691 (2018) 401–407.

[27] D. M. Mitnik, J. Randazzo, G. Gasaneo, Endohedrally confined helium: Study of mirror collapses, Physical Review A 78 (2008) 062501.

Figures

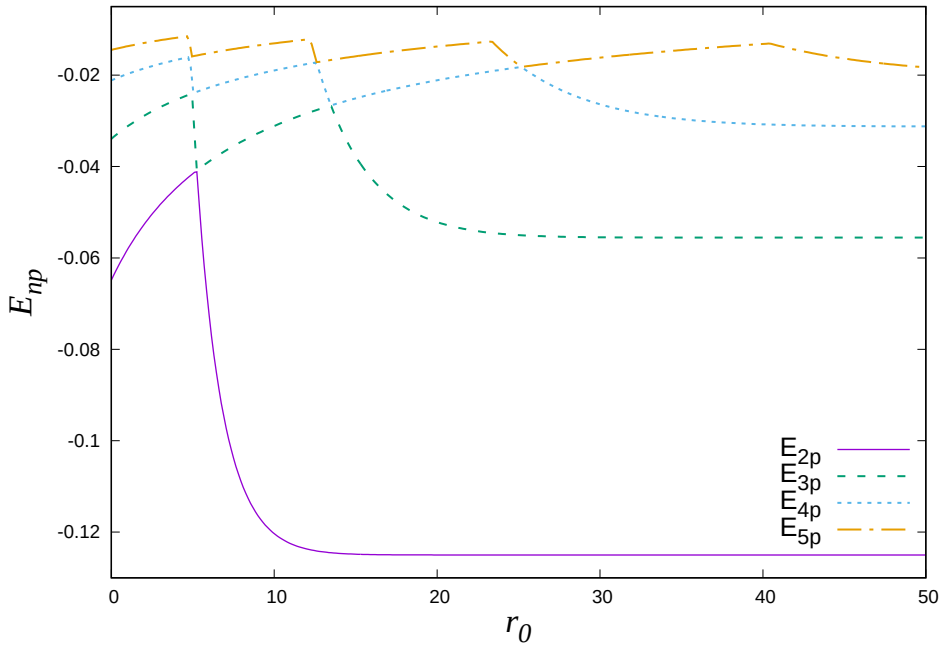

Figure 1: Energy of the confined $2p$ to $5p$ states as a function of the confinement size, r_0.

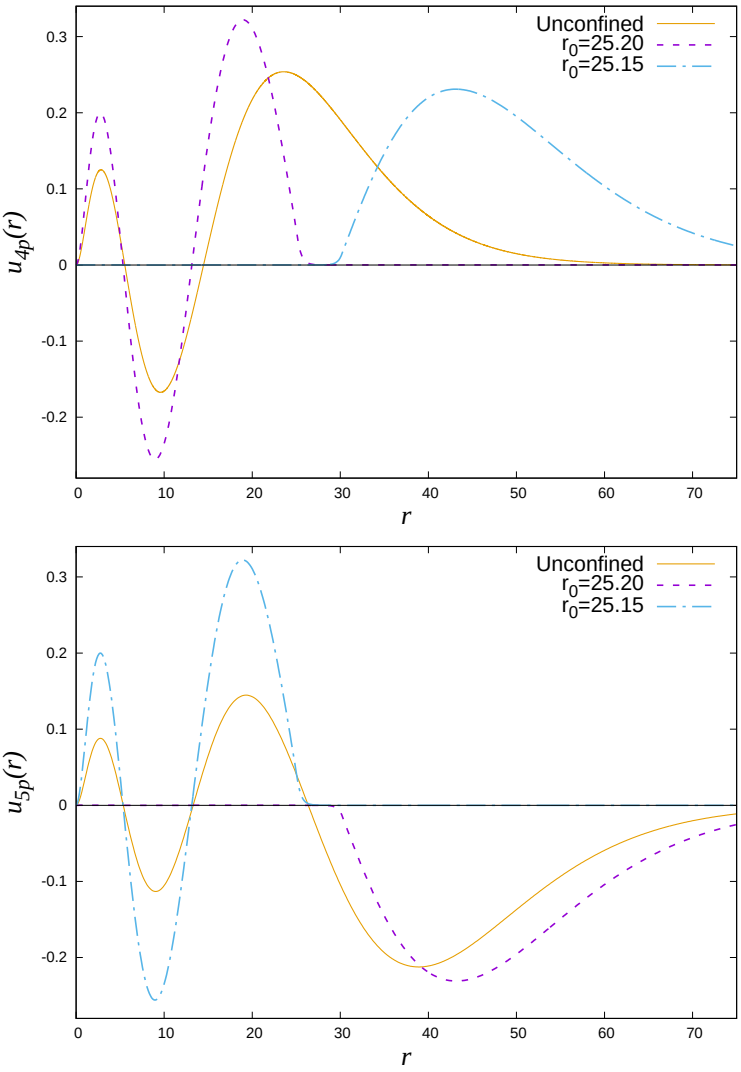

Figure 2: Upper panel: Reduced radial functions, $u(r)$, of the confined $4p$ state for confinement sizes of $r_0 = 25.15$ and $r_0 = 25.2$. The unconfined radial orbital is also shown. Lower panel: The same for the $5p$ state.

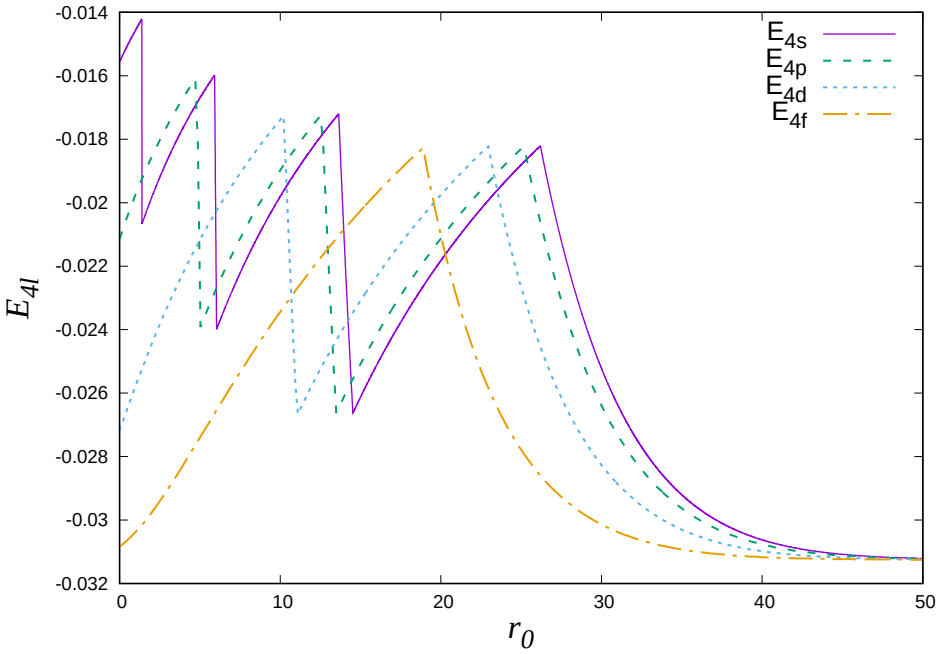

Figure 3: Energy of the confined $4s$ to $4f$ orbitals as a function of r_0.

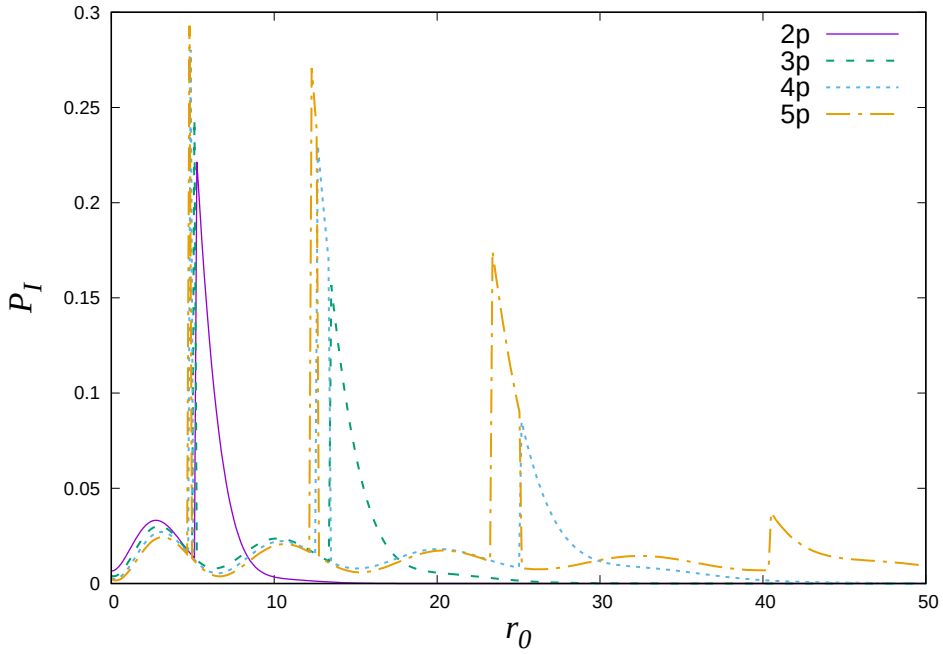

Figure 4: Ionisation probability of the $2p$ to $5p$ orbitals as a function of r_0.

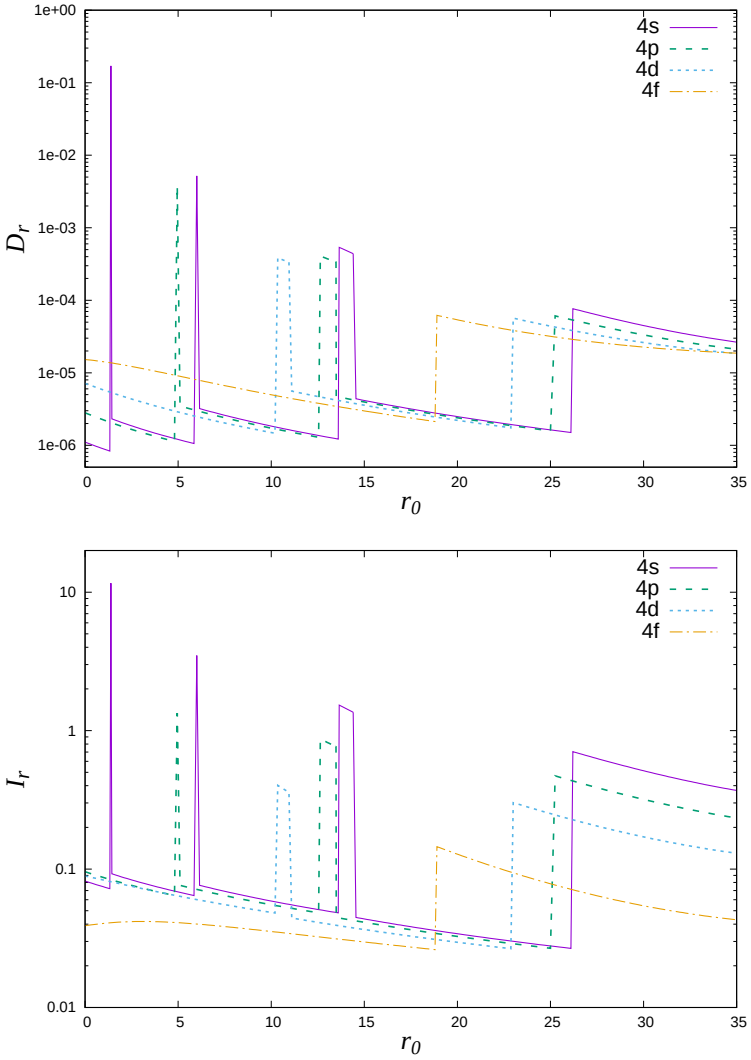

Figure 5: Upper panel: Disequilibrium, D_r, in log scale for the $4s$ to $4f$ states as a function of r_0. Lower panel: The same for the Fisher information index, I_r.

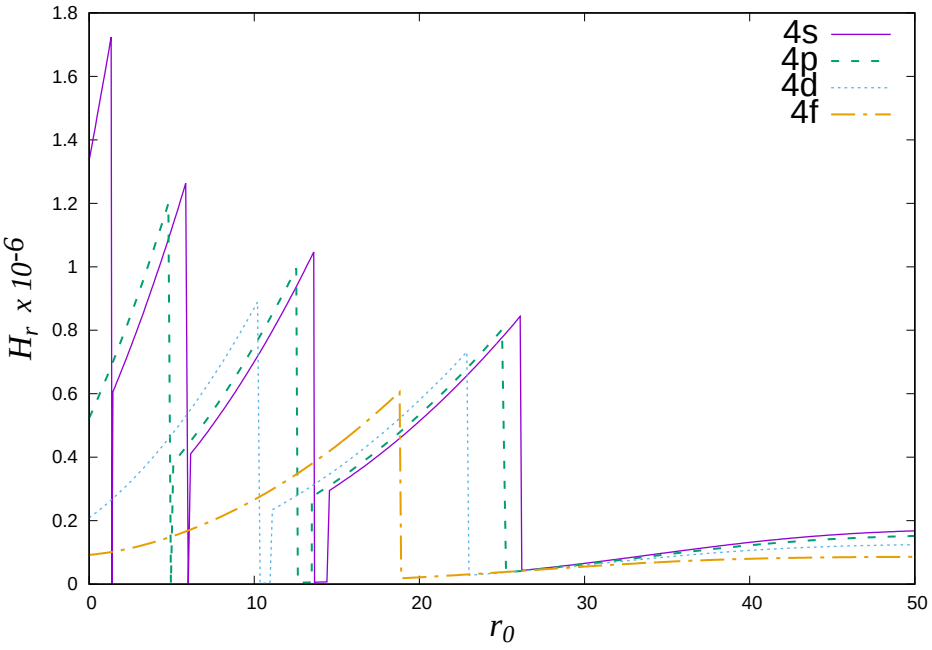

Figure 6: Exponential Shannon information entropy, H_r, for the $4s$ to $4f$ states as a function of r_0.

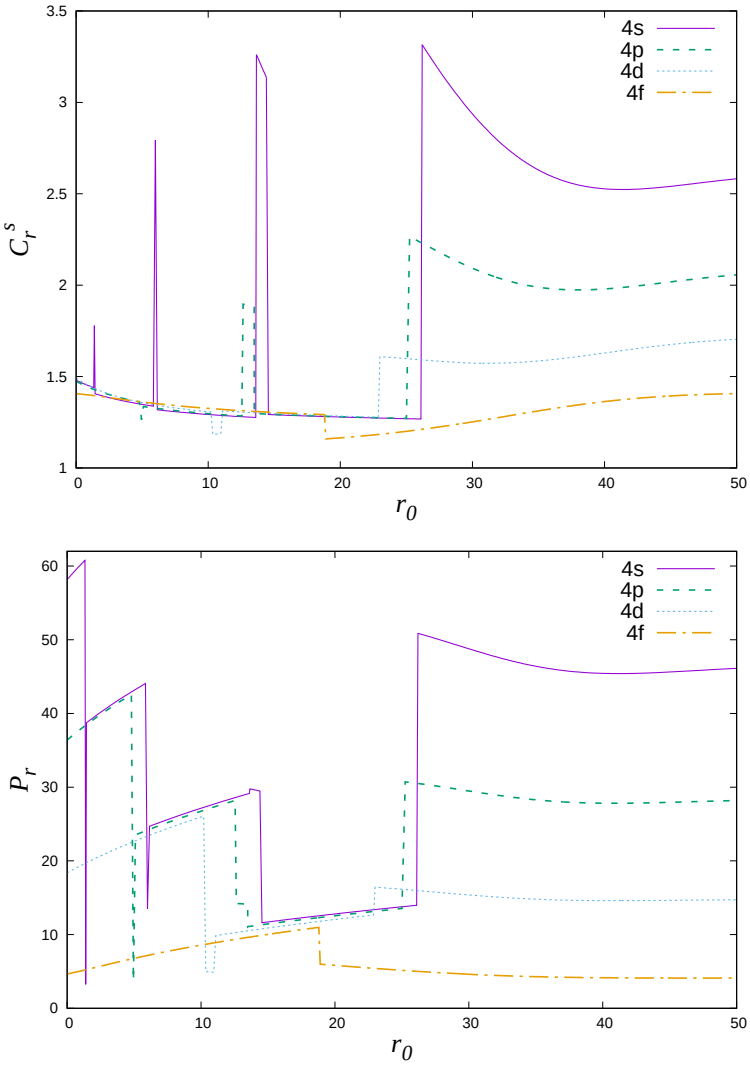

Figure 7: Upper panel: Shape LMC complexity index, C_r^s, for the $4s$ to $4f$ states as a function of r_0. Lower panel: FS complexity index, P_r, for the same orbitals as a function of r_0.